Calculated electric field gradients and electronic properties of acceptors in CdTe

S. Lany, V. Ostheimer, H. Wolf and Th. Wichert
Technische Physik, Universität des Saarlandes, D-66041 Saarbrücken, Germany

Linearised augmented plane wave (LAPW) calculations are performed in order to determine the electric field gradients (EFG) induced by group V and group Ib acceptors in CdTe at the nearest neighbour (NN) atomic site. Experimentally, the EFG are measured by the perturbed γγ-angular correlation spectroscopy using the radioactive probe isotopes ^{111}In and ^{77}Br. Besides the identification of the experimentally observed defects, the LAPW calculations provide information about fundamental properties of the EFG. For the group Ib acceptors, the dependence of the EFG on the NN distance is opposite to the expectation from the simple point charge model.

1. Introduction

Measured by different experimental techniques, such as perturbed γγ-angular correlation (PAC), Mössbauer spectroscopy, or nuclear quadrupole resonance, defect-related electric field gradients (EFG) in semiconductors have been successfully used as 'fingerprints' of the respective defects in the past, because the EFG is very sensitive to an anisotropic charge distribution about the probe nucleus, caused for example by a neighbouring defect [1, 2]. The EFG discussed in this paper are experimentally determined by PAC spectroscopy, using the radioactive PAC probe atoms ^{111}In and ^{77}Br. In the II-VI semiconductor CdTe, both ^{111}In and ^{77}Br are donor atoms which can form close donor-acceptor (D-A) pairs with stable acceptors, driven by the Coulomb attraction of ionised donors and acceptors. Thus, $^{111}In_{Cd}$ donors form nearest neighbour (NN) pairs with group V acceptors located at the Te sublattice, and $^{77}Br_{Te}$ donors form NN pairs with group Ib acceptors located at the Cd sublattice. The actual PAC measurement takes place after the radioactive decay of the parent probes ^{111}In and ^{77}Br at the $I = 5/2$ excited state of the daughter isotopes ^{111}Cd and ^{77}Se, respectively, and yields the quadrupole coupling constant ν_Q, related to the EFG by $\nu_Q = |eQV_{zz}/h|$, along with the asymmetry parameter $\eta = (V_{xx}-V_{yy})/V_{zz}$ ($|V_{xx}| \le |V_{yy}| \le |V_{zz}|$). The component V_{zz} is calculated from ν_Q using the quadrupole moments $Q = 0.83$ b for ^{111}Cd [3] and $Q = 0.76$ b for ^{77}Se [4]. Exemplified for the group V acceptor N and the group Ib acceptor Ag, the local defect structure after the radioactive decay of the PAC probes is sketched in fig. 1.

In the present work, the linearised augmented plane wave (LAPW) code WIEN97 [5] is employed for EFG calculation. Exchange and correlation effects are treated in the generalized gradient approximation as described in Ref. [6] being a development based on the local density approximation (LDA). The general treatment of a defect in a semiconductor host lattice within this method is performed according to Ref. [7], where a BCC supercell with a 32 atom basis and the tetrahedral symmetry of the T_d point-group was used for the calculation of the group V acceptors. Here, we are dealing also with cases in which two impurity atoms are introduced into the supercell and consequently a trigonal symmetry (C_{3v}) is present.

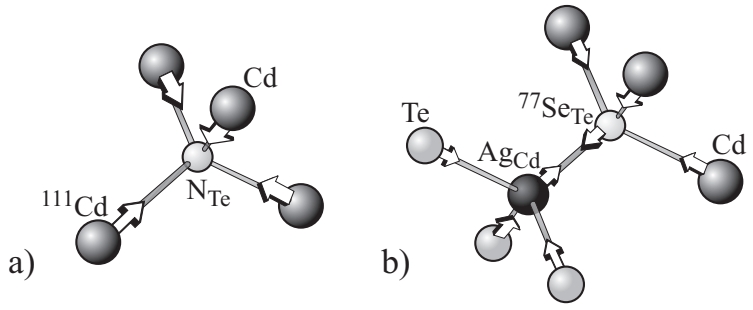

Fig. 1. Local defect structure after the radioactive decay of the parent PAC probe. (a) N acceptor trapped at a ^{111}In donor which decays to ^{111}Cd (T_d symmetry). (b) Ag acceptor trapped at a ^{77}Br donor which decays to ^{77}Se (C_{3v} symmetry). Arrows indicate structural relaxation.

Table 1. Experimental EFG, calculated EFG, and calculated NN distance of the probe-defect pair for group V and group Ib acceptors in CdTe. The calculated EFG refer to the ionised acceptors (e.g. N_{Te}^-) and to the NN-Cd and the NN-Se_{Te} site, respectively. The NN distance of the undisturbed CdTe lattice is d_{NN} = 2.81 Å.

	experiment	theory	
	V_{zz} [10^{21}V/m^2]	V_{zz} [10^{21}V/m^2]	d_{NN} [Å]
^{111}Cd-N_{Te}^-	±13.95(5)	–13.7	2.20
^{111}Cd-P_{Te}^-	±10.56(9)	–11.2	2.50
^{111}Cd-As_{Te}^-	±9.27(5)	–9.5	2.57
^{111}Cd-Sb_{Te}^-	±7.62(5)	–8.1	2.71
$^{77}Se_{Te}$-Cu_{Cd}^-	±5.3(2)	–3.6	2.46
$^{77}Se_{Te}$-Ag_{Cd}^-	±6.7(2)	–6.7	2.64
$^{77}Se_{Te}$-Au_{Cd}^-	±2.6(3)	–1.1	2.64

2. Results of EFG calculations

PAC experiments yield characteristic, axially symmetric EFG ($\eta = 0$) for the ^{111}Cd-(group V) [8] and the ^{77}Se-(group Ib) [9] pairs (T_M = 295 K). In the case of the Au acceptor, however, the PAC spectrum measured with the probe ^{77}Br/^{77}Se is difficult to analyse, because less than a whole modulation period is obtained. Assuming an axially symmetric EFG as observed for the Cu and Ag acceptors, the quadrupole coupling constant ν_Q = 47(4) MHz is obtained which is unexpectedly small for a NN pair. However, the PAC spectrum can also be described reasonably by a damped fit function modelling an EFG distribution about zero caused by a disturbed lattice environment. Thus, the support for the interpretation of the experimental data by the EFG calculations is highly appreciated.

In table 1, the calculated EFG for the ionised group V and group Ib acceptors are compared to the experimental data, taking into account the lattice relaxation about the defect complex in the LAPW calculation. The axial symmetry of the EFG tensor in the EFG calculations is constrained by the applied T_d and C_{3v} symmetry. Additionally, the calculated distance d_{NN} between the acceptor and the PAC probe is listed in table 1. For the group V acceptors, the agreement of the theoretical and experimental EFG is excellent, the difference is within about 0.5×10^{21}V/m^2. For the group Ib acceptors, the calculated EFG differ from the experimental values by 1.7×10^{21}V/m^2 at maximum, which still confirms the proposed defect model, i.e. the observation of $^{77}Se_{Te}$-Cu_{Cd}, $^{77}Se_{Te}$-Ag_{Cd}, and $^{77}Se_{Te}$-Au_{Cd} complexes. (Note that absolute differences between calculated and experimental EFG should be regarded rather than relative ones, because V_{zz} can assume negative and positive values including zero. Experimentally, the sign of V_{zz} is not determined.) In particular, the unusually low magnitude of the EFG the Au acceptor is causing at a NN site is clearly reproduced. The somewhat larger differences to the experimental data compared to the group V acceptors are probably due to the well known limitations of the LDA in describing moderately localized *d* electrons, i.e. the outer *d* shell of the group Ib elements in the present case. For both the group V and the group Ib acceptors, the calculated value of V_{zz} in the neutral state of the acceptor yields less agreement with the experimental data. Consequently, the measured EFG are attributed to the ionised state.

3. The distance dependence of the EFG

The calculated EFG is very sensitive to the actual distance between the acceptor site and the site of the probe atom (Cd or Se_{Te}) at which the EFG is determined. If this distance is shortened by only 1% of the bond length of the undisturbed CdTe lattice, the EFG already changes considerably: The EFG at a NN Cd neighbour to a group V acceptor changes by about $\Delta V_{zz} = -0.9\times10^{21}$ V/m^2, while the EFG at a Se_{Te} site caused by a neighbouring group Ib acceptor changes by about $\Delta V_{zz} = +0.4\times10^{21}$ V/m^2. Thus, taking into account lattice relaxa-

tion is crucial for EFG calculation. For the Se_{Te}-(group Ib) pairs, the positive ΔV_{zz} for a decreasing NN distance together with the negative values for V_{zz} (see table 1) result in the surprising observation that the *absolute value* of the EFG at the Se_{Te} probe site *decreases* with decreasing distance from the group Ib acceptor. The simple point charge model, in which the ionised acceptor represents a point charge causing the EFG, is incapable to explain this behaviour. The point charge model can reasonably be applied to highly ionic crystals [10], but obviously it breaks down in the case of covalent bonding present in semiconductors. Speaking in terms of the electron orbitals of the chemical bonds, the EFG is generally dominated by the *p* contribution of the valence electrons, and often the EFG is in good approximation proportional to the anisotropy of the partial *p* charge [11]:

$$V_{zz} \sim \tfrac{1}{2}(p_x + p_y) - p_z \qquad (1)$$

For both the group V and the group Ib acceptors, the influence of lattice relaxation on the EFG is analysed in more detail by means of calculations with an artificial displacement of the four NN atoms. Since the above mentioned distance dependence of the EFG at the Se_{Te} site holds analogously for a Te site neighboured to an isolated group Ib acceptor, and in this case the higher T_d symmetry can be employed, the EFG at a Te site instead of a Se_{Te} site is considered in the following. For two NN distances, d_{NN} = 2.65 Å and d_{NN} = 3.03 Å, the EFG at a NN-Cd and a NN-Te site is plotted in fig. 2 for the As_{Te}^{-} and the Ag_{Cd}^{-} acceptor, respectively (solid lines). The pure relaxation effect is determined by calculating the EFG in the absence of the acceptor impurity and changing the distance of the four NN atoms to the central host atom (fig. 2, dashed lines). The linear interpolation between the two representative NN distances in fig. 2 was checked to be a good approximation within the considered range of d_{NN}.

A remarkably strong EFG at a Cd site is obtained if the four NN Cd atoms are moved to or from the central Te atom (fig. 2, Cd-Te pair). This EFG is in the same order of magnitude as the defect induced EFG (cf. the Cd-As_{Te} pair) and arises due to the rearrangement of the electronic charge after the relaxation; e.g. for an inward relaxation the Cd-p_z partial charge is increased with respect to the Cd-p_{xy} charge leading to a negative V_{zz} according to eq. (1) (the local *z* axis is understood to direct towards the central Te atom). For the Cd-As_{Te} pair, the slope of the graph in fig. 2 is almost the same as for the Cd-Te pair, indicating that the charge rearrangement induced by relaxation is similar in both cases. As a further discrepancy to the point charge model, the EFG of the Cd-As_{Te} pair changes the sign at $d_{NN} \approx 2.9$ Å. The pure relaxation effect at the Te site (fig. 2, Te-Cd pair) is less pronounced than for the Cd site, but qualitatively similar. In contrast to all other cases, the slope of the graph for the Te-Ag_{Cd} pair in fig. 2 is negative, indicating that the EFG of the group Ib acceptors is affected in a specific way during the relaxation, leading to the unexpected distance dependence.

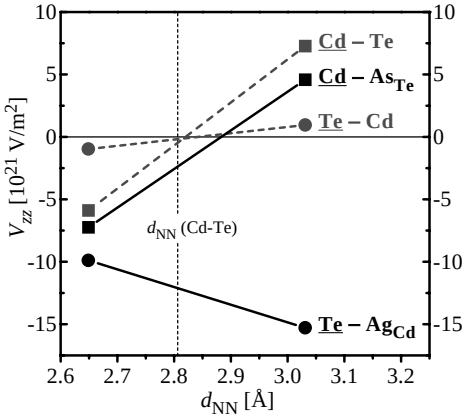

Fig. 2. The EFG as a function of the NN distance for the ionised As and Ag acceptor and for the pure CdTe crystal, in which the host atoms are artificially displaced. The atomic site at which the EFG is determined is underlined.

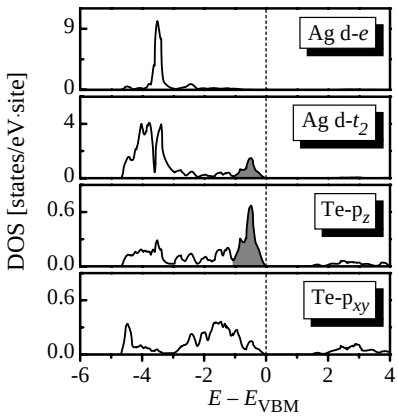

Fig. 3. Site projected, angular momentum decomposed DOS. The interaction between the Ag *d*-t_2 and the Te-p_z states is indicated by a shading of the respective DOS region.

4. The influence of the group Ib *d* electrons

Besides the unusual distance dependence of the EFG, a further puzzling observation is the weak EFG for the Au acceptor, in particular compared to the Ag acceptor having the identical calculated NN distance to the Se_{Te} probe (see table 1). For both effects, the *d* electrons of the group Ib elements play an important role: In the crystal field of a semiconductor with zincblende structure, such as CdTe, the atomic *d* orbital splits into non-degenerate t_2 and *e* sublevels. Additionally, the group Ib *d* electrons can interact with the Te-*p* electrons (or Se_{Te}-*p* electrons, analogously), where for symmetry reasons only the *d*-t_2 sublevel and the Te-p_z orbitals are affected. For the isolated Ag_{Cd} acceptor, fig. 3 shows the electronic states decomposed into the t_2 and *e* symmetries of the Ag-*d* electrons and the p_z and p_{xy} symmetries of the NN Te-*p* electrons. The *d*-t_2 and *d*-*e* levels are located about 4 eV below the valence band maximum (VBM), but the *d*-t_2 symmetry shows up an additional peak at the energy of the Te-p_z state ($E_{VBM} - 0.5$ eV, cf. shading in fig. 3). As a consequence of this *p*-*d* interaction, Te-p_z like charge is transferred to the Ag *d*-t_2 charge, and the EFG at the Te (or Se_{Te}) site becomes weaker [i.e. V_{zz} becomes more positive according to eq. (1)] than it would be in the absence of the Ag-*d* electrons. Thus, the considerably weaker EFG for the Au acceptor compared to the Ag acceptor is understandable: Due to the additional core electrons and the 4*f* shell, the Au-5*d* shell is more extended than the Ag-4*d* shell, and the overlap with the Te-*p* states is even larger. Consequently, the Te-p_z to Au *d*-t_2 charge transfer is more pronounced and the EFG at the Te (Se_{Te}) site is weaker for Au than for Ag. The distance dependence can be explained by the fact that the *p*-*d* interaction fades out for increasing NN distances and the charge transfer becomes smaller, leading to a stronger EFG, i.e. a more negative V_{zz}.

5. Summary

In order to support the identification of defects, LAPW calculations are performed which yield defect related EFG for Cd-(group V) and Se_{Te}-(group Ib) pairs in CdTe. In particular for the Au acceptor, where the experimental situation is ambiguous, a clear interpretation is achieved only by support of the EFG calculation. For the group Ib acceptors, an analysis of the electronic structure reveals the influence of the outer *d* electrons on the EFG and the origin of the unexpected dependence of the EFG on the NN distance. Thus, besides the theoretical prediction of the EFG, the LAPW calculations provide insight into the electronic structure of defect complexes in semiconductors.

The financial support of the Bundesministerium für Bildung und Forschung (BMBF) under Contract No. 03WI4SAA is gratefully acknowledged.

References

[1] Hyperfine Interaction of Defects in Semiconductors, ed. G. Langouche, Amsterdam, 1992.
[2] Th. Wichert, in: Identification of Defects in Semiconductors, ed. M. Stavola, Semiconductors and Semimetals Vol. 51B, Academic Press, San Diego, 1999, p. 297.
[3] P. Herzog, K. Freitag, M. Rauschenbach, H. Walitzki, Z. Phys. A 294(1980)13.
[4] P. Blaha, P. Dufek, K. Schwarz, H. Haas, Hyperfine Int. 97/98(1996)3.
[5] P. Blaha, K. Schwarz, J. Luitz, WIEN97, A Full Potential Linearized Augmented Plane Wave Package for Calculating Crystal Properties (K. Schwarz, Techn. Universität Wien, Austria), 1999. ISBN 3-9501031-0-4.
[6] J.P. Perdew, S. Burke and M. Ernzerhof, Phys. Rev. Lett. 77(1996)3865.
[7] S. Lany, P. Blaha, J. Hamann, V. Ostheimer, H. Wolf and Th. Wichert, Phys. Rev. B 62(2000)R2259.
[8] V. Ostheimer, A. Jost, T. Filz, St. Lauer, H. Wolf and Th. Wichert, Appl. Phys. Lett. 69(1996)2840.
[9] V. Ostheimer, S. Lany, H. Wolf and Th. Wichert, to be published.
[10] R.N. Attili, M. Uhrmacher, K.P. Lieb, L. Ziegler, M. Mekata and E. Schwarzmann, Phys. Rev. B 53(1996)600.
[11] K. Schwarz, C. Ambrosch-Draxl and P. Blaha, Phys. Rev. B 42(1990)2051.